Estimation of initial-state structures in high-energy heavy-ion collisions using principal component analysis

Shreyasi Acharya[*] and Subhasis Chattopadhyay[†]
Variable Energy Cyclotron Centre, HBNI, 1/AF, Bidhan Nagar, Kolkata 700064, India

(Received 27 November 2020; accepted 8 March 2021; published 29 March 2021)

In high-energy heavy-ion collisions, structures in the initial collision zone are a matter of intense investigation, both from theory and experimental points of views. A large number of models have been developed to represent the initial state of the collision including the Glauber model and color glass condensate (CGC), among others. Another important aspect of the study is to investigate proper observables that will be sensitive to the initial collision zone. In this work, we discuss a formalism to implement the spatial clusters at the partonic level in the string melting version of the AMPT model for PbPb collisions at $\sqrt{s_{NN}} = 200$ GeV. These clusters are then propagated through the AMPT hadronization scheme. Principal component analysis (PCA) has been used on the η, ϕ, and p_T distributions of the produced charged particles and the eigenvalues have been compared before and after the implementation of the clustering. It is found that for all these three different distributions, all the prominent PCA modes show sensitivity to the clustering. A centrality dependent study has also been performed on those eigenvalues.

DOI: 10.1103/PhysRevC.103.034909

I. INTRODUCTION

In heavy-ion collisions at ultrarelativistic energies at the Relativistic Heavy Ion Collider (RHIC) and the Large Hadron Collider (LHC), corresponding to a medium of high temperature, a state of strongly interacting medium is formed in which partons are deconfined from the incoming hadrons. A range of observables that are measured to characterize the properties of the medium include thermodynamic properties such as temperature and entropy, collective properties given by flow parameters, and gluon density of the medium measured by jet quenching, among others. It is a usual practice that the experimental observables are theoretically evaluated by folding the space-time evolution of the colliding medium to find the sensitivity to the different stages of the evolution [1,2]. The prominent stages that are modeled include initial state of the collision, formation of the medium, evolution and cooling of the medium, hadronization, rescatterings, chemical and kinetic freeze-out, and finally the free streaming of particles. In the initial stage of the collision, when nucleons overlap, the geometry of the collision zone plays a crucial role in determining the final state observables [3]. It has been observed that the final state collectivity parameters commonly known as flow parameters are correlated with the initial state geometry or corresponding fluctuations. These initial state geometry parameters, such as various orders of eccentricities from coordinate space (ϵ_n), leave their imprints on the azimuthal distributions of the momentum of the produced particles. The decompositions of the azimuthal distributions are represented by parameters of various orders such as v_1, v_2, etc. as obtained by the Fourier decomposition of the azimuthal distributions with respect to the reaction plane angle [4,5]. The degree of conversion of the initial spatial asymmetry to the final state momentum asymmetry is represented by the correlation between the eccentricities of the flow parameters. To study such an effect, one needs to evaluate the event-by-event eccentricities and hadronic flow parameters. It is, however, important to investigate in detail the effect of these initial state geometry parameters or their fluctuations on the distributions of the final-state observables such as pseudorapidity or transverse momentum distributions of the produced particles. In the literature, a range of models describing high-energy heavy-ion collisions have been discussed that include specific structures of the initial state geometry due to nucleonic overlap or formation of new structures at the partonic or hadronic levels in the form of clusters. Prominent examples include the parton cascade model (PCM) [6], color glass condensate (CGC) [7], and Zhang's parton cascade (ZPC) [8], among others. It is a usual practice to implement different initial state scenarios before evolution of the medium using ideal or viscous hydrodynamics, and a conclusion is made about the suitable description of the initial state that matches the data best. Efforts are also made to study the sensitivity to the fluctuations in the initial state using various methods such as sensitivity to the final state observables [9–11]. In the present study, we have implemented a clustering algorithm on partons formed by the AMPT model [12] in PbPb collisions at RHIC energy. The clustering algorithm has been motivated by the formation of spatial domains consisting of thermal partons. These partons are then processed via the hadronization scheme in the string-melting version of AMPT, which is based on the recombination mechanism. The final state particles are then studied in detail.

[*]shreyasi.acharya@gmail.com
[†]sub@vecc.gov.in

In the literature, distributions of the produced particles are analyzed using various decomposition methods, such as Fourier analysis applied on the azimuthal distributions in order to extract the flow parameters. Recently, principal component analysis (PCA) has been used extensively, primarily to study various orders of flow variables and their correlation with the initial geometry parameters and their fluctuations [13]. There are two main approaches applied in the field of high-energy heavy-ion collisions for the PCA decomposition. The first one is the decomposition of the covariance of the azimuthal distributions weighted with a Fourier series and then making connection of the PCA components with the flow parameters [14]. Another approach is to decompose the inclusive distributions using PCA and connect the components with the physical observables such as flow parameters in the case of decomposition of the azimuthal distributions. Nowadays PCA is being used extensively in automated machine learning procedures for finding structures in object spaces. The features primarily detected using PCA are then analyzed using sophisticated cluster finding algorithm to obtain the features in detail. In our study, we have adopted the latter approach, i.e. decomposing the inclusive distributions and studying the components. The initial clustering might introduce features in η, ϕ, p_T space such as flow coefficients in the azimuthal distribution. As the eigenvalues are sensitive to these features, we can choose a region of eigenvalues that will select the events considered.

We discuss the AMPT model and the PCA procedure as applied in our study in Secs. II and III respectively. We then discuss the procedure of implementation of clustering in Sec. IV, results in Sec. V, and the summary in Sec. VI.

II. AMPT

A Multi-Phase Transport (AMPT) [12] is a Monte Carlo partonic transport model being used widely for simulating NN, NA, and AA collisions at high energy. The model implements all major stages of the collision starting from the initial state through the partonic scattering followed by hadronization and hadronic rescattering. The initial stage of the collision has been implemented by HIJING [15] through Monte Carlo–Glauber model calculations in NA and AA collisions. In the initial state of the collisions, either partonic strings and minijets are taken together from HIJING or all strings are melted into partons. There are two versions of AMPT: in the default version, only the minijets are transported using Zhang's parton cascade (ZPC), and, in the string melting version, all melted partons go through ZPC for scattering. The scattering is governed by a parameter to be tuned to match the particle spectra. The hadronization is implemented in two modes known as hadronic mode and partonic mode. In hadronic mode, minijets, after scattering, are recombined with the strings and then get fragmented using Lund's string fragmentation model. On the other hand, in the partonic mode, all the partons combine to form hadrons (mesons or baryons) based on the spatial distance, spin structures, and the invariant mass of the quarks (quark-antiquark in the case of mesons and three quarks in case of baryons). The hadrons formed by any of these two mechanisms then undergo scattering among themselves and then scattered hadrons reach the detector. AMPT has been used extensively in high-energy heavy-ion collisions and has been able to explain most of the observables such as spectra and flow, among others. One extremely prominent finding of the model is the ability to explain the number of constituent quark (NCQ) scaling of elliptic flow parameter v_2 at RHIC. The NCQ scaling refers to the scaling behavior observed when the v_2 and p_T of different identified hadrons are divided by the number of constituent quarks (n_q). The v_2/n_q vs p_T/n_q for identified hadrons follow a universal curve suggesting the dominance of quark degrees of freedom at the early stages of collisions. In our study, we have used only the partonic version of the model involving partons at the initial stage and in hadronization. At the initial stage, a separate partonic clustering was implemented, as discussed in Sec. IV.

III. PRINCIPAL COMPONENT ANALYSIS (PCA)

PCA is a method of decomposing a correlated distribution in various components known as principal components that reflect the independent variables characterizing the features of the distributions. PCA is essentially a procedure of dimension reduction from correlated matrix with the eigenvalues representing the variance.

Mathematically, a matrix $(N \times m)$ can be decomposed as

$$M = X\Sigma Z = VZ, \tag{1}$$

where X, Z are orthogonal matrices of dimensions $N \times N$ and $m \times m$ respectively, and Σ is a diagonal matrix of dimensions $N \times m$ with diagonal elements arranged in strictly decreasing order. These elements carry physical meaning. In our case, the distribution of a variable in an event can be expressed as

$$f = \sum_{j=1}^{m} x_j^{(i)} \sigma_j z_j = \sum_{j=1}^{(i)} v_j^{(i)} z_j, \tag{2}$$

where z_j is an orthogonal vector such that $Z_i^T x Z_j = \delta_{ij}$, σ_j are the diagonal elements of matrix Σ, index i represents the event number $(1, 2, \ldots, N)$, and m is the number of bins of the input variable. $v_j^{(i)}$ is the corresponding coefficient of z_j for the ith event. In PCA, σ_j are obtained in decreasing order and only the top few values are enough to describe the distribution, say up to k, then we can rewrite the equation above as

$$f = \sum_{j=1}^{k} v_j^{(i)} z_j, \tag{3}$$

where j are PCA modes describing the fluctuations in the distribution.

PCA has been used so far mostly for analyzing the covariance of the azimuthal distributions of the produced particles as weighted by a Fourier series, primarily to extract the flow coefficients [16–18]. The PCA components represent flow fluctuations in different orders and nonlinear couplings among the flow coefficients. In another approach, however, the inclusive azimuthal distributions are decomposed by PCA and it is found that the eigenvectors of at least up to fourth order are similar to the distributions of the Fourier components. The eigenvectors have been found to be of shapes similar to

those of the Fourier components, as used in the conventional method of extraction of the flow coefficients. The eigenvalues have been found to correspond to the flow coefficients. If applied at the partonic level, the eigenvalues of PCA correspond to the eccentricities (ϵ_n) of various orders. The flow coefficients of various orders have been interpreted as being connected to the initial spatial geometry and their fluctuations as being transferred to the momentum-space anisotropy. Flow coefficients (v_n) follow a linear relationship with their corresponding initial state eccentricities (ϵ_n) [14,19]. In earlier studies using PCA for the azimuthal distributions, event-by-event v_n's have been extracted and then correlated with ϵ_n. In the present study, event-by-event distributions for η, ϕ, p_T have been divided into n bins separately. The exercise is then undertaken for a large number (N) of events. Such binned distributions per event along with the number of events form a matrix to be diagonalized. The eigenvalues are obtained in a strictly decreasing order.

In our study, η, ϕ, and p_T distributions of the produced charged particles are decomposed separately for events having initial geometry with and without inclusion of additional clustering. The main aim of this study is to investigate the behavior of the eigenvalues with the changes in the initial conditions. It has been argued elsewhere that the eigenvalues of PCA correspond to the fluctuations in various orders [20]. With the modified initial conditions, the fluctuations are expected to change and the PCA eigenvalues should be sensitive to these changes. In conventional approaches, events with high PCA eigenvalues could be extracted and those events could be further investigated using sophisticated cluster-finding methods to find the substructures in the set of events. This approach is used in machine learning techniques quite extensively. The PCA method in its current form uses the covariance among the data to obtain the results; however, the approach is not limited to the second-order cumulant only. A multivariate cumulant study via their principal components was first proposed by [21], analogous to the usual principal components of a covariance matrix. This cumulant method of principal component analysis has been used in various fields of research such as mathematics, economics, and computer science.

IV. IMPLEMENTATION OF CLUSTERING

In the literature, there is a series of models which have implemented the initial states of high-energy heavy-ion collisions; a few prominent models that include different initial conditions are NUXUS [22], EPOS [23], MC-KLEIN [24], and IP-GLASMA [25], among others. In the present work, we have implemented clusters at the partonic level, which is basically inspired by the discussions on formation of spatial domains at the partonic level.

We started with the partons from the AMPT string melting version and implemented the clustering in the following way. A parton, selected as a seed at random, is taken as the center of a cluster. All partons whose interparton distance with respect to the seed parton lie within a certain cluster radius (parameter R) are assigned as members of that cluster.

The cluster is then formed by bringing the partons closer to the center by reducing the radial distances of the partons

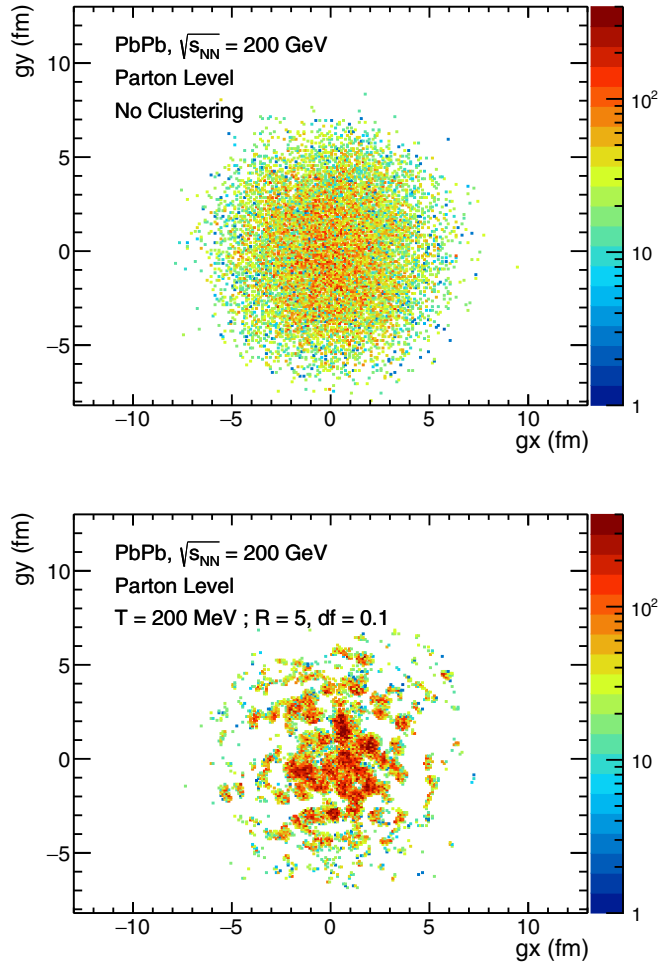

FIG. 1. X-Y distribution of the partons before (top) and after (bottom) clustering.

by a certain factor (parameter df). Once the formation of one cluster is completed, another unassigned parton is taken as a seed and the process continues till all partons are exhausted.

The next step is to implement a momentum distribution of the members of the partonic cluster. Motivated by the thermally distributed partons, the cluster partons have been assigned momenta according to the distribution

$$f(p_T) = e^{-p_T/T} \tag{4}$$

where, T is a parameter analogous to the temperature of the cluster. In our study, we have used T values of 200 and 400 MeV. Figure 1 shows the X-Y distribution of the partons on the transverse plane before (top) and after (bottom) clustering. The clustering parameters for the plot are $R = 5$ fm, $df = 0.1$, $T = 200$ MeV. As seen in the figure, while before clustering (top) the position distributions of the partons are uniform, clear domain structures are seen in Fig. 1 (bottom), which could be said to correspond to the partonic domains in the position space. Please note that with these parameters, the clusters correspond to maximum radii of 0.5 fm ($R \times df$).

Figure 2 shows the η, ϕ, and p_T distributions of the initial partons before and after the clustering with two different temperature parameters and different spatial cluster

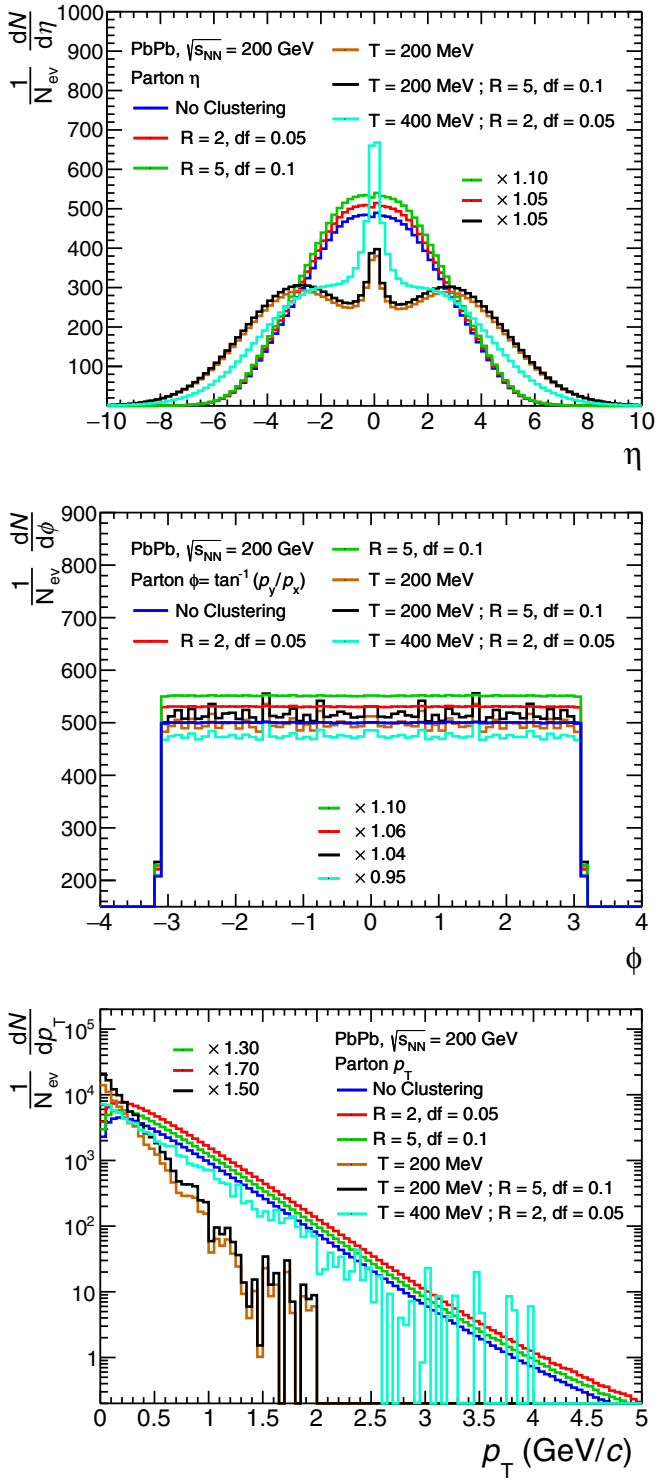

FIG. 2. η, ϕ, and p_T distributions of the partons before and after clustering for minimum-bias PbPb collisions at $\sqrt{s_{NN}} = 200$ GeV.

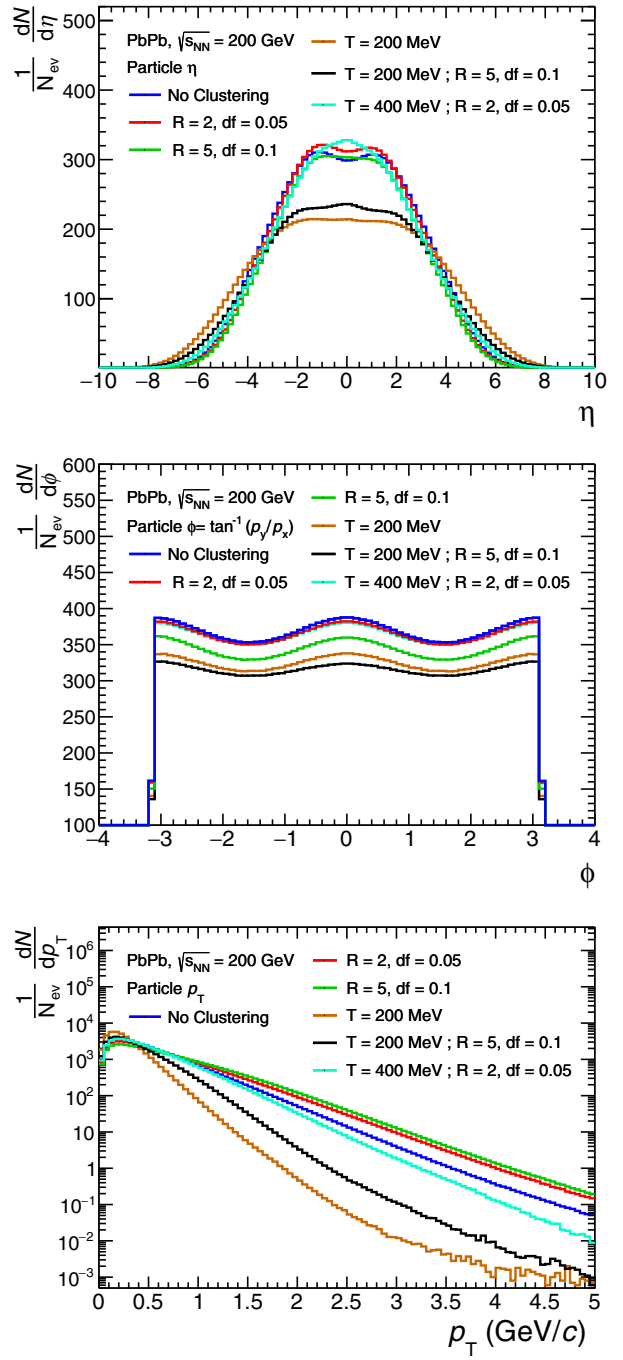

FIG. 3. η, ϕ, and p_T distributions of the produced particles before and after clustering for minimum bias PbPb collisions at $\sqrt{s_{NN}} = 200$ GeV.

parameters. Three cases of clustering were considered in the figure: The legends where only T values (200 or 400 MeV) are mentioned are cases where the parton momentum was distributed according to Eq. (4) and no position clustering was implemented. Legends where T, R, and df values are mentioned are the ones where both position clustering was implemented and parton momentum was assigned according to Eq. (4). Finally, the ones with only R and df values and no temperature values are cases where only position clustering was applied and momentum was not changed. The η, ϕ and p_T distributions obtained after applying the aforementioned changes were compared with the case where no changes in position and momentum were made. The η distribution of partons changes from a uniform to a peaking shape at $\eta = 0$, which represents the formation of the clusters. The

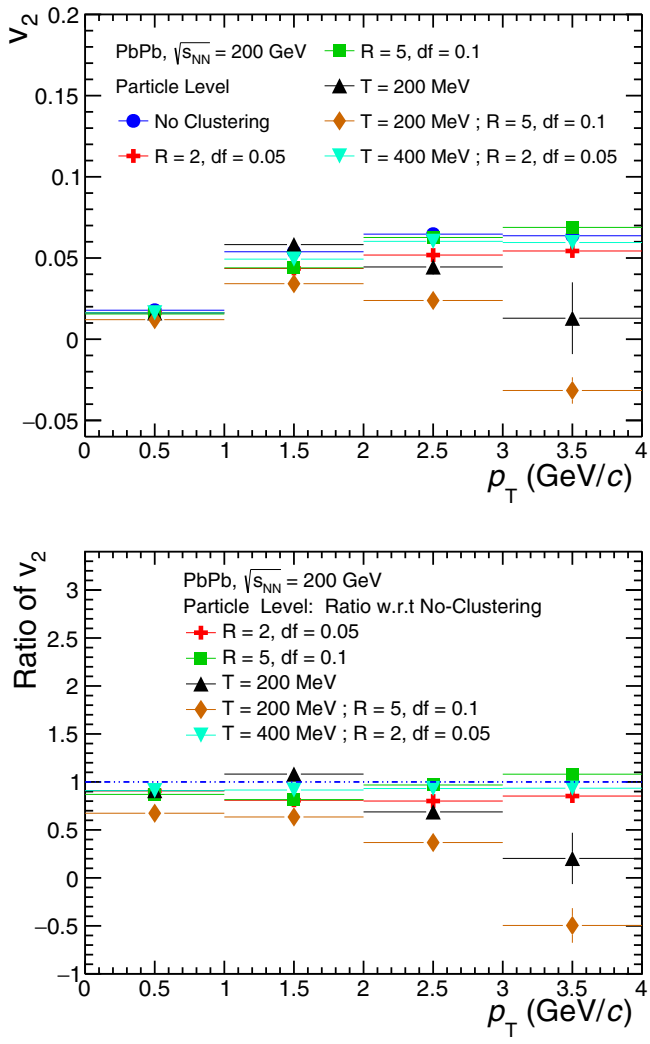

FIG. 4. p_T distributions of v_2 for two scenarios, i.e., before and after clustering (upper panel) and the ratio of v_2 vs p_T distributions after clustering with respect to the one before.

η distributions for similar temperature parameters overlap, e.g., the no-clustering and only position clustering overlap, as the momentum has not been changed, while the two curves with $T = 200$ MeV overlap. For better visibility of the plots some of the overlapping curves have been scaled as shown in the legends. The azimuthal distributions are mostly uniform except for a few hints of azimuthal asymmetry/structure in the clusters which have undergone momentum modification and, as expected, p_T distributions depict the modified distribution according to the value of the input T parameter. Similar to the η distributions in the p_T distributions, curves with similar temperature and similar transverse momentum distributions overlap. The partons then undergo scattering using ZPC and hadronization as implemented in the partonic version of AMPT, i.e., the coalescence of quarks and antiquarks. We have shown the corresponding distributions of the produced charged particles in Fig. 3. It is seen that all characteristic structures seen at the partonic level are smoothed out. The azimuthal distributions of the produced particles on the other hand show the characteristic asymmetric shape due to elliptic flow. The p_T range of the produced particles increases as compared to that of partons due to the production of hadrons consisting of more than one parton.

V. RESULTS

In this study, we have performed simulations using AMPT string-melting version for PbPb collisions at $\sqrt{s} = 200$ GeV. We generated up to 2×10^5 minimum bias events and ensured that the statistical errors on the event averaged eigenvalues are not significantly large. We used only the results from the produced charged particles in this study. As discussed earlier in Sec. III, we divided each eventwise distribution into 20 bins for the η and p_T distributions in the regions of -1 to $+1$ for η and 0 to 5 GeV/c for p_T, and 50 bins in the region $-\pi$ to $+\pi$ for ϕ. Before discussing the PCA results, we first obtained the elliptic flow parameter v_2 using the event plane method [26] for two cases, i.e., with and without clustering. The cluster parameters have been varied to represent different possibilities. In Fig. 4 and the subsequent figures, we have opted for two values of the cluster radius parameter (R), i.e., 2 and 5 fm associated with parameter values $df = 0.05$ and 0.1 respectively. For cases without any mention of the temperature parameters T, parton momenta remain unmodified compared to those from AMPT. For clusters having thermal partons, the T parameters chosen are 200 and 400 MeV. Note that, for partons with no clustering, the fitted slope of the p_T spectra gives an inverse slope of about 400 MeV. The clusters with $T = 200$ MeV therefore represent significantly softer partons.

Figure 4 (top) shows the variation of v_2 with p_T for two scenarios. As seen in Fig. 4 (top), v_2 increases with p_T except for $T = 200$ MeV, in which v_2 decreases at higher p_T. We have also shown the ratio of v_2 in Fig. 4 (bottom) taking the no-clustering scenario as reference and, as discussed earlier, the ratio remains constant at unity is thereby insensitive to the clustering except in the $T = 200$ MeV case.

As mentioned earlier, the eigenvalues of PCA are related to the eccentricities at the partonic level and various flow components and their fluctuations as obtained from the azimuthal

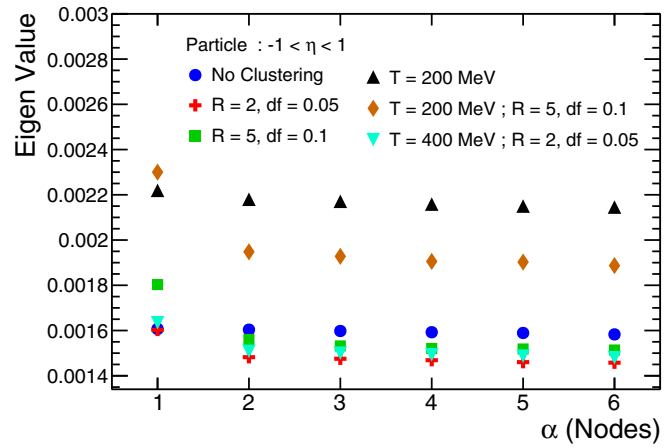

FIG. 5. Eigenvalues as obtained for η distribution before and after clustering.

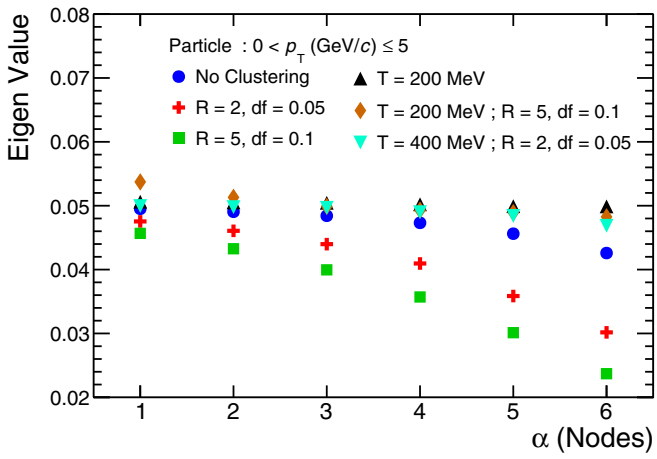

FIG. 6. Eigenvalues as obtained for p_T distribution before and after clustering.

distributions at the particle level. We have investigated the eigenvalues for different distributions of the charged particles with different cluster parameters. Figures 5, 6, and 7 show the distributions of the eigenvalues as obtained for η, ϕ, and p_T distributions for two different scenarios, i.e., with and without clustering. The nodes (α) in the x axis represent the PCA components. It is clear in all cases that the most prominent eigenvalue is that of the first component, differing from the next one by varying degrees. It can therefore be mentioned that the first eigenvalue, representing the variance of the distribution of the reduced dimension, can be used further for investigating the structures in the initial state of the collision zone.

According to the PCA method, eigenvalues are arranged in decreasing order, sometimes with a wide difference between the eigenvalue of a component and that of the next node. Before discussing PCA results, we reexamine Figs. 2 and 3 showing the inclusive distributions of partons and of the produced charged particles respectively. It is clearly seen that, among partonic η and ϕ distributions, structures are more prominent for the η distributions, presumably due to the inclusion of clustering at the partonic level. However, at the particle level, no such structures are prominently visible. In view of this, it is important to study the PCA eigenvalues at the particle level with and without clustering.

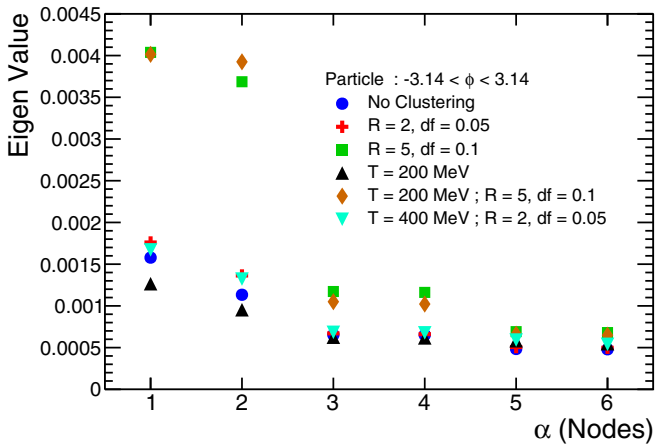

FIG. 7. Eigenvalues as obtained for ϕ distribution before and after clustering.

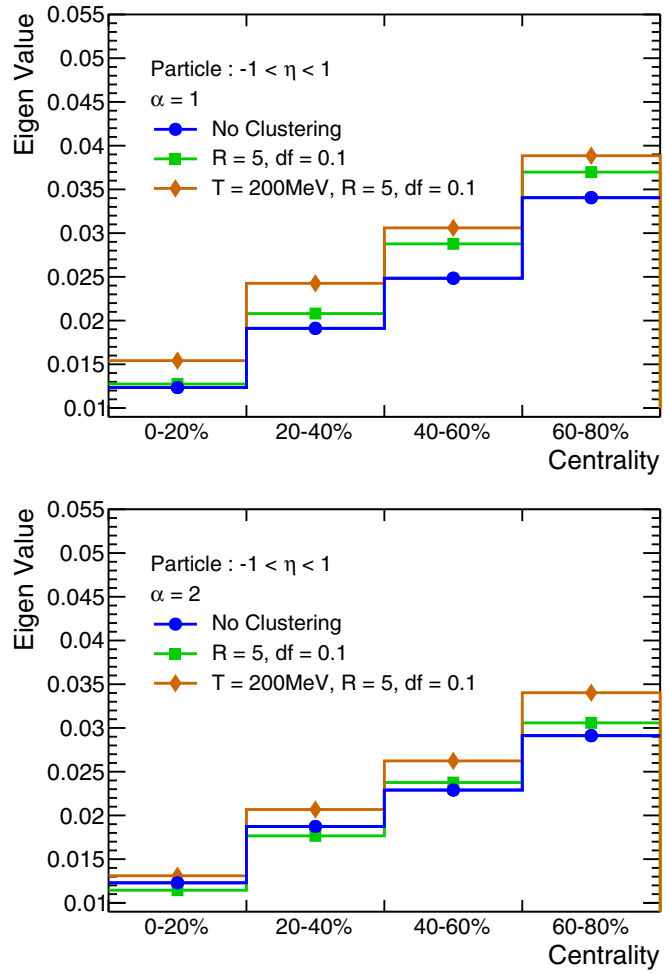

FIG. 8. Eigenvalues as obtained for η distribution before and after clustering.

For the p_T distribution, the position clustering lowers the eigenvalues compared to the no-clustering case while the clusters including thermal partons tend to increase the eigenvalues for all nodes. The same pattern is also seen in the η distributions, with the exception of the first node ($\alpha = 1$), where cases involving clustering with $R = 5$ fm have a higher eigenvalue than the no-clustering scenario. In case of the ϕ distributions, eigenvalues are seen closer in pairs presumably representing the real and imaginary components of the flow parameters [14]. We have not made any detailed investigation of extraction of flow parameters from these eigenvalues. We only point out that the eigenvalues differ clearly for the two cases, i.e., with and without clustering. We have also observed a clearer effect of the position clustering in the case of ϕ as eigenvalues for $R = 5$ fm lie considerably higher compared to the no-clustering values. The eigenvalues

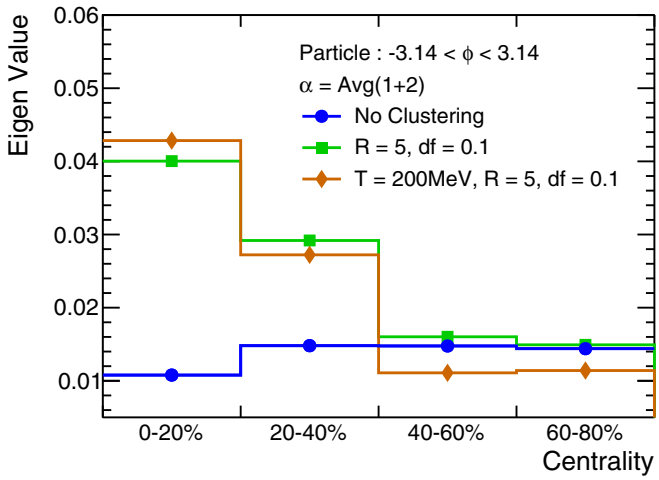

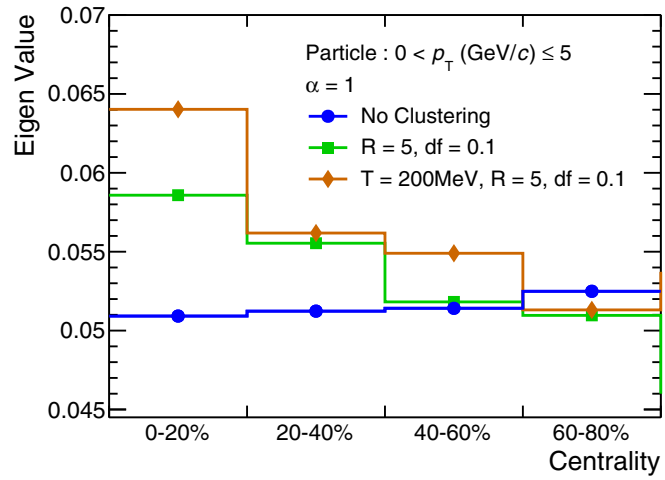

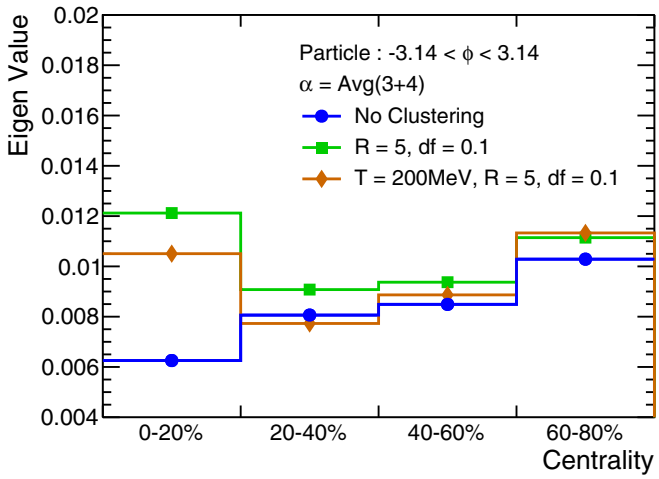

FIG. 9. Eigenvalues as obtained for ϕ distribution before and after clustering.

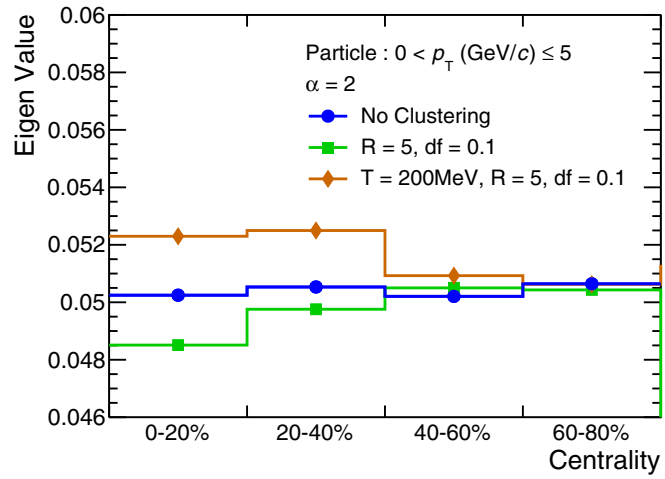

FIG. 10. Eigenvalues as obtained for p_T distribution before and after clustering.

of the ϕ distributions look more sensitive to the position clustering.

We have also performed studies for various event centralities. Figures 8 to 10 show the variation of the eigenvalues of two different modes (1 and 2) with event centralities. We have only taken two cases that showed maximum effect in earlier eigenvalue studies, i.e., (i) $R = 5$ fm, $df = 0.1$, and no momentum modifications and (ii) $T = 200$ MeV, $R = 5$ fm, and $df = 0.1$. It is seen that the eigenvalues of the first component for the ϕ and p_T distributions have a decreasing trend for the events where clustering is implemented as compared to the events without clustering.

The observed decreasing trend of the first eigenvalues might be due to higher fluctuations for lower multiplicities in peripheral events. No significant structures are seen for the η distributions of the produced particles in both the cases. It is also seen that the eigenvalues are considerably lower in the case of minimum-bias events as shown in the Figs. 5–7 and discussed earlier. This might be due to dilution of fluctuations for minimum-bias events due to the admixture of events with different multiplicities.

VI. SUMMARY AND CONCLUSIONS

In an effort to find a method to investigate the initial partonic structure in high-energy heavy-ion collisions, we have implemented the formation of partonic clusters using the partons obtained from the string-melting version of the AMPT model. The clusters are formed in two steps: first by bringing partons closer in positions to an extent defined by two parameters, i.e., the radius of the partonic zone (R) and the scaling factor on the interpartonic distance. In our work, we have used the values $R = 2$ and 5 fm and $df = 0.05$ and 0.1. Additionally, we have introduced a thermal distribution to the cluster partons by tuning the temperature parameters; we have used two temperature values, i.e., $T = 200$ MeV and $T = 400$ MeV. The latter one is close to the inverse slope of the p_T distribution from the AMPT partons. These partons then undergo hadronization by the AMPT string-melting hadronization scheme, i.e, by coalescence of partons according to their distance, spin, and mass. We then investigated the distributions of the produced particles from AMPT in order to find the sensitivity of the particle-level observables to the partonic structures. Even though the structures are reflected in basic

distributions of the partons, there is no clue of these structures in the inclusive distributions of the produced particles. For this investigation, we have used principal component analysis (PCA) to analyze the η, ϕ, and p_T distributions of the produced particles. It may be mentioned that the square root of the sum of the squares of the paired eigenvalues from the azimuthal distribution of a particular order has been shown to be related to the coefficients of flow up to v_6 [14]. In our work we have taken the eigenvalues as our candidate for probing the initial state at different clustering conditions. For our study, we have looked into the eigenvalues obtained from PCA decomposition of η, ϕ, and p_T distributions as our observables and looked at them for various conditions such as no clustering, only position clustering, and inclusion of thermal partons with $T = 200$ and 400 MeV. It is found that the first few prominent eigenvalues for all three distributions are sensitive to the inclusion of clustering. For η and p_T distributions, two clear groups are seen lying above and below the no-clustering scenario. For $T = 200$ MeV, all eigenvalues lie above the no-clustering reference. For position clustering, the eigenvalues are grouped below the reference. It is seen that the difference with the no-clustering reference is more for higher values of the R parameter. For the azimuthal distributions, the eigenvalues of which are related to the flow parameters, it appears that the sensitivity higher towards the position clustering. We have also studied the centrality dependence of the first two eigenvalues. Even though the η values do not show appreciable sensitivity, for ϕ and p_T, they a show clearly different trend as compared to the no-clustering reference, which is mostly flat. We therefore conclude that the first few eigenvalues are sensitive to the inclusion of domains at the partonic level. The events with domains might be identified on an event-by-event basis by discriminating based on the eigenvalues. It is already known that the eigenvalues of the azimuthal distributions represent the flow parameters. In general the PCA eigenvalues represent fluctuations in the distributions of different orders, which are not visible in the inclusive distributions; however, further analysis using the PCA might be performed to extract the physical interpretations of the eigenvalues and eigenvectors from the η and p_T distributions.

ACKNOWLEDGMENT

We would like to thank the VECC grid computing facility for helping in performing the computing for this work. We also acknowledge the funding from the Department of Atomic Energy, Govt. of India.

[1] J. Adams *et al.* (STAR Collaboration), Nucl. Phys. A **757**, 102 (2005).
[2] K. Adcox *et al.* (PHENIX Collaboration), Nucl. Phys. A **757**, 184 (2005).
[3] J.-Y. Ollitrault, Phys. Rev. D **46**, 229 (1992).
[4] S. Voloshin and Y. Zhang, Z. Phys. C **70**, 665 (1996).
[5] U. Heinz and R. Snellings, Annu. Rev. Nucl. Part. Sci. **63**, 123 (2013).
[6] B. Muller, Int. J. Mod. Phys. E **12**, 165 (2003).
[7] F. Gelis, E. Iancu, J. Jalilian-Marian, and R. Venugopalan, Annu. Rev. Nucl. Part. Sci. **60**, 463 (2010).
[8] B. Zhang, Comput. Phys. Commun. **109**, 193 (1998).
[9] H. Petersen, C. Coleman-Smith, S. A. Bass, and R. Wolpert, J. Phys. G **38**, 045102 (2011).
[10] C. E. Coleman-Smith, H. Petersen, and R. L. Wolpert, J. Phys. G **40**, 095103 (2013).
[11] S. Floerchinger and U. A. Wiedemann, Phys. Rev. C **88**, 044906 (2013).
[12] B. Zhang, C. M. Ko, B.-A. Li, and Z.-W. Lin, Phys. Rev. C **61**, 067901 (2000).
[13] R. S. Bhalerao, J.-Y. Ollitrault, S. Pal, and D. Teaney, Phys. Rev. Lett. **114**, 152301 (2015).
[14] Z. Liu, W. Zhao, and H. Song, Eur. Phys. J. C **79**, 870 (2019).
[15] M. Gyulassy and X.-N. Wang, Comput. Phys. Commun. **83**, 307 (1994).
[16] A. Mazeliauskas and D. Teaney, Phys. Rev. C **91**, 044902 (2015).
[17] A. M. Sirunyan *et al.* (CMS Collaboration), Phys. Rev. C **96**, 064902 (2017).
[18] P. Bozek, Phys. Rev. C **97**, 034905 (2018).
[19] B. Alver and G. Roland, Phys. Rev. C **81**, 054905 (2010); **82**, 039903(E) (2010).
[20] I. T. Jolliffe and J. Cadima, Philos. Trans. R. Soc. A **374**, 20150202 (2016).
[21] J. Morton and L.-H. Lim, Principal cumulant component analysis preprint, 2009, http://galton.uchicago.edu/∼lekheng/work/pcca.pdf
[22] H. J. Drescher, M. Hladik, S. Ostapchenko, T. Pierog, and K. Werner, Phys. Rep. **350**, 93 (2001).
[23] T. Pierog, I. Karpenko, J. M. Katzy, E. Yatsenko, and K. Werner, Phys. Rev. C **92**, 034906 (2015).
[24] H. J. Drescher and Y. Nara, Phys. Rev. C **75**, 034905 (2007).
[25] B. Schenke, P. Tribedy, and R. Venugopalan, Phys. Rev. Lett. **108**, 252301 (2012).
[26] A. M. Poskanzer and S. A. Voloshin, Phys. Rev. C **58**, 1671 (1998).